Liquid Crystals
Publication details, including instructions for authors and subscription information:
http://www.informaworld.com/smpp/title~content=t713926090

Groove depth dependence of the anchoring strength of a zero order grating-aligned liquid crystal

B. T. Hallam[a]; J. R. Sambles[a]
[a] Thin Film Photonics, School of Physics, University of Exeter, Stocker Road, Exeter EX4 4QL, UK,

Online publication date: 06 August 2010

To cite this Article Hallam, B. T. and Sambles, J. R.(2000) 'Groove depth dependence of the anchoring strength of a zero order grating-aligned liquid crystal', Liquid Crystals, 27: 9, 1207 — 1211
To link to this Article: DOI: 10.1080/02678290050122051
URL: http://dx.doi.org/10.1080/02678290050122051

LIQUID CRYSTALS, 2000, VOL. 27, NO. 9, 1207–1211

Groove depth dependence of the anchoring strength of a zero order grating-aligned liquid crystal

B. T. HALLAM* and J. R. SAMBLES

Thin Film Photonics, School of Physics, University of Exeter, Stocker Road, Exeter EX4 4QL, UK

(*Received 19 November 1999; in final form 27 February 2000; accepted 20 March 2000*)

The influence of in-plane electric fields on the twist profile of a liquid crystal aligned by non-diffractive (zero order) gratings has been explored using an optical guided mode technique. The liquid crystal is studied in a novel cell geometry comprising one rubbed polyimide alignment layer and one zero order diffraction grating. Comparison of the director-distorted profiles with predictions from elastic continuum theory allow both the twist elastic constant of the bulk liquid crystal and the azimuthal anchoring strengths at the two surfaces to be determined. Experiments have been performed on different depth gratings. Good agreement with the Berreman topological alignment model has been achieved for fairly shallow gratings, but not for gratings with deeper groove profiles. This implies that the theory needs modification to account for deep gratings.

1. Introduction

Alignment of liquid crystal directors by grating-like surfaces has attracted considerable attention [1–13] over the years. Recent devices based on grating alignment have demonstrated good viewing angle characteristics [8] and bistability [9]. However, the exact mechanism of the alignment remains a debated topic. Some authors suggest it is topological in nature [1], while others claim it is molecular in nature [3, 12]. The proposed topological model considers the free energy of liquid crystal directors aligned parallel and perpendicular to the grooves that form the grating profile [1]. An expression for the azimuthal (in-plane) anchoring strength (W_a) is then derived in terms of the liquid crystal elastic constant (k) and the amplitude (a) and pitch (λ_g) of the grating:

$$W_a = \frac{2\pi a^2 k}{\lambda_g^3}. \tag{1}$$

Despite the model assumptions, there have been reports of good agreement with experimentally determined anchoring strengths on diffraction gratings [11, 13], although the authors of [13] invoked surface memory effects to account for the liquid crystal elastic constant required in the analysis.

Here we present an optical guided mode study of a series of liquid crystal cells aligned with different depth zero order diffraction gratings. By applying an in-plane electric field, the liquid crystal director profile is distorted. These distortions are quantified by analysing angle-dependent Fully Leaky Guided Mode (FLGM) [14] data, and are compared with predictions from an elastic continuum model. The anchoring energy for gratings with different depths is determined. These are reviewed in the context of the Berreman topological model.

*Author for correspondence; e-mail: bthallam@exeter.ac.uk

2. Theory and experimental details

Since a full mathematical treatment of the theory and experiment are given elsewhere [15–17], only the pertinent points have been listed here.

(1) A Frank–Oseen free energy equation with Rapini–Papoular type anchoring at the surfaces may be used to describe a nematic liquid crystal.

(2) Twist deformation of the liquid crystal under application of an in-plane electric field is governed by the Euler–Lagrange equation:

$$\frac{d^2\phi}{dz^2} = -\frac{\varepsilon_0 \Delta\varepsilon \mathbf{E}^2}{k_{22}} \sin\phi \cos\phi \tag{2}$$

where $\phi = \phi(z)$ is the twist angle of the nematic, z is the direction through the cell thickness, $\mathbf{E}$ is the electric field magnitude applied across the in-plane electrode gap and $\Delta\varepsilon$ is the dielectric anisotropy of the material.

(3) This equation may be solved for the boundary conditions supplied by the torque-balance equations assuming both a finite anchoring strength on each surface, equations (3) and (4), and a zero-field

twist through the cell, equations (5) and (6).

$$k_{22}\left(\frac{d\phi}{dz}\right)_{z=d/2,\phi=\phi_{d1}} = 2W_{a1}(\phi_{o1}-\phi_{d1}) \quad (3)$$

$$k_{22}\left(\frac{d\phi}{dz}\right)_{z=-d/2,\phi=-\phi_{d2}} = 2W_{a2}(\phi_{o2}-\phi_{d2}) \quad (4)$$

$$k_{22}\left(\frac{\phi'_{o1}+\phi'_{o2}}{d}\right) = 2W_{a1}(\phi_{o1}-\phi'_{o1}) \quad (5)$$

$$k_{22}\left(\frac{\phi'_{o1}+\phi'_{o2}}{d}\right) = 2W_{a2}(\phi_{o2}-\phi'_{o1}) \quad (6)$$

where, ϕ_{o1} and $-\phi_{o2}$ are the easy axes of alignment, ϕ'_{o1} and $-\phi'_{o2}$ are the actual twist angles of the directors at each surface, ϕ_{d1} and $-\phi_{d2}$ are the surface twist angles under application of the electric field, and d is the cell thickness.

(4) Optical guided mode analysis allows the zero field director profile and cell thickness to be determined. Using this, together with the dielectric anisotropy ($\Delta\varepsilon$) of the liquid crystal and the applied field strength, the twist profile of the director through the cell can be generated by choosing different values of the twist elastic constant (k_{22}) and the azimuthal anchoring strengths (W_{a1} and W_{a2}) at each surface.

(5) A multilayer optical theory is used to generate model angle-dependent reflectivity and transmission data from this twist profile.

(6) Optimizing the values for k_{22}, W_{a1} and W_{a2} allows a best fit to be obtained to experimental data at different field strengths.

The cell geometry used in this study is shown in figure 1. In-plane gold electrodes (350 nm thick, 3 mm electrode spacing) were evaporated onto one of the substrates prior to spin deposition (at 3500 rev s^{-1} for 35 s) of polyimide. Having been baked for 3.5 h, the polyimide

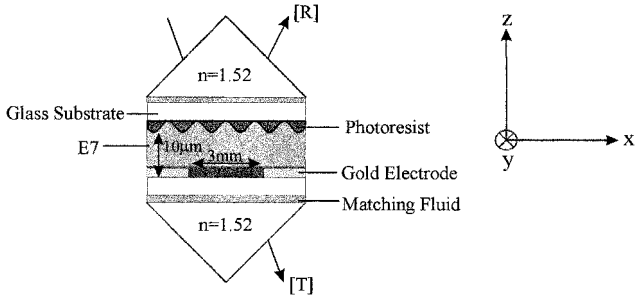

Figure 1. A slice (in the incidence plane) through the experimental cell geometry. Alignment of the liquid crystal is homogeneous and is close to parallel to the electrode edges. Standard-index glass prisms are optically matched to the cell by a silicone oil matching fluid.

was carefully rubbed along the direction of the electrode edges with a velvet covered rolling-drum. A second substrate was prepared by spin deposition of photoresist (Shipley 1805) at 3000 rev s^{-1} for 60 s. Interferographic exposure [18] with radiation from a helium-cadmium ($\lambda_0 = 325$ nm) laser produced a zero order grating with a pitch of 176.2 nm. This value was verified by a Littrow-angle scan of the grating in the ultraviolet. Varying the exposure times produced a series of gratings with the same pitch, but with different depths. These depths were deduced from polarization conversion measurements [19].

The two substrates were arranged so that the grating groove direction was the same as the rubbing direction; beaded glue provided a plate spacing of about 6 μm. Cell filling of the nematic liquid crystal E7 took place under vacuum in the isotropic phase, which was subsequently slowly cooled into the nematic phase to ensure a good monodomain with the surface directors observed to be parallel to the rubbing direction and groove direction. The exact deviation (if any) of the surface director from the grating groove direction could not be obtained, because the grating was designed to be non-diffractive at all visible wavelengths. Hence a precise observation of the groove orientation through the direction of propagation of the diffracted orders was not possible. Since the cell was constructed from standard index glass, the observation of diffracted orders via ultraviolet illumination through the back face of the cell was also prohibited. However, alignment was observed to be parallel to the groove direction by eye (the grating orientation was carefully marked during the manufacture process).

Light-coupling prisms were optically matched onto the cell with silicone oil index matching fluid. The cell was then placed in a temperature-stable environment on the centre of rotation of a rotating table and illuminated with light from a HeNe (632.8 nm) laser. A set of eight angle-dependent reflectivity and transmission data was recorded. Two polarizers allowed the incident (first subscript) and detected (second subscript) polarization states to be set. These eight data sets comprise reflection (R) and transmission (T): R_{pp}, R_{ps}, R_{sp}, R_{ss}, T_{pp}, T_{ps}, T_{sp} and T_{ss}. By fitting these data to multilayer optical theory, the zero field director profile may be established. A weak 10 kHz a.c. electric field was then applied across the electrode gap, and data were recorded for several different field strengths ($\mathbf{E}_{max} < 3.0 \times 10^{-2}$ V μm^{-1}).

3. Results and discussion

The complexity of modelling the surface of the zero order grating was reduced by dividing the grating and interfacial liquid crystal into two discrete planar layers.

The first of these layers was isotropic to represent the bulk photoresist. The second was anisotropic (with refractive indices intermediate between those of the liquid crystal and the photoresist) to represent the grating/liquid crystal interfacial region. This is a fair approximation since the grating features are small (groove width ~ 88 nm) and hence do not contribute any losses into diffracted orders. When modelling the field-distorted profiles, the liquid crystal layer was divided into 100 layers. This ensured that the modelled profile was a smooth function on the scale of the wavelength of light.

Figure 2 shows typical fits of angle-dependent reflectivity and transmission data (symbols) to multilayer optical theory (solid line). The data are collected with s-polarized light incident and detected, and the grating has a depth of (62 ± 8) nm.

Having obtained the zero-field director profile, a suitably twist-sensitive azimuthal angle for the cell was chosen by examining the effects of small in-plane twists on the modelled reflectivity and transmission intensities. It is at this cell azimuth that the applied voltage data were collected. Figure 3 shows the effects of various weak 10 kHz a.c. electric fields on the transmitted polarization conversion signal (T_{ps}). Again the experimental data are shown as symbols and the theory as a solid line. To obtain these fits, at a temperature of 21°C, a value of $\Delta\varepsilon = 13.91$ [15] was used. A twist elastic constant of $(6.5 \pm 0.08) \times 10^{-12}$ N was experimentally determined. This is in good agreement with results from light-scattering experiments [20]. The average anchoring strength on the rubbed polyimide surface was experimentally determined to be $(1.3 \pm 0.1) \times 10^{-4}$ J m^{-2} where the error has been obtained through observing the tolerance of the fit to changes in the relevant parameter. The maximum deviation of the experimentally determined values of W_a for individual polyimide surfaces from this average value is 7%. This discrepancy is easy to understand since all the cells were constructed

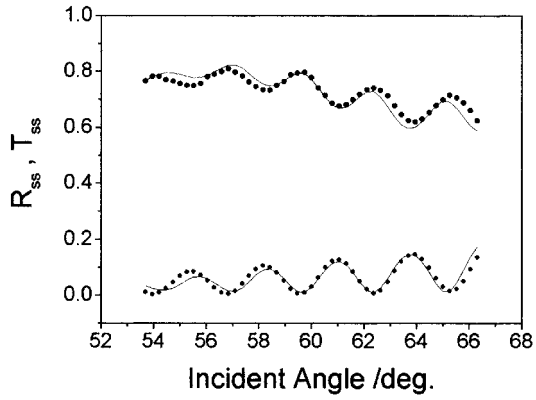

Figure 2. Typical fits (solid lines) to angle-dependent polarization conservation data (symbols).

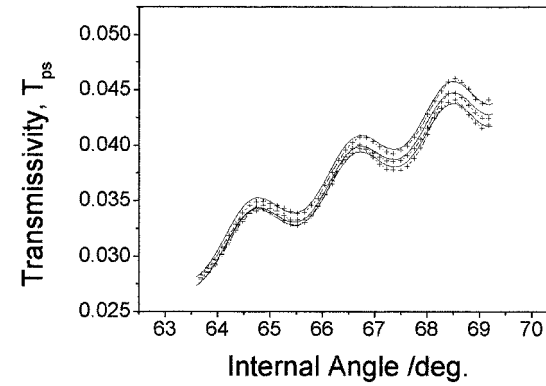

Figure 3. The effect of an in-plane a.c. field (0, 100, 140 V_{rms} across a 3 mm electrode gap) on the transmission signal T_{ps} at 21.0°C. Experimental data are shown as crosses and the theory as a solid line.

using different polyimide-coated substrates, each of which was prepared at a different time using the same (largely uncontrollable) rubbing strength. Hence this 7% variation in W_a on the rubbed polyimide surfaces is due to the slightly different rubbing conditions experienced by each sample in our rubbing machine. (The authors would like to stress that this 7% variation in W_a is an artefact of the laboratory rubbing machine and is almost certainly not representative of the tolerance associated with the rubbing process in industrial plants where large plates of glass are treated. These large glass sheets may subsequently be cut to form many cells with very little difference between the surface properties associated with each.) Values determined for the anchoring strength on each of the grating surfaces are plotted as symbols on figure 4. A solid line that corresponds to the predictions from Berreman's theory, equation (1), has also been plotted. This line is not intended as a line of best fit, but

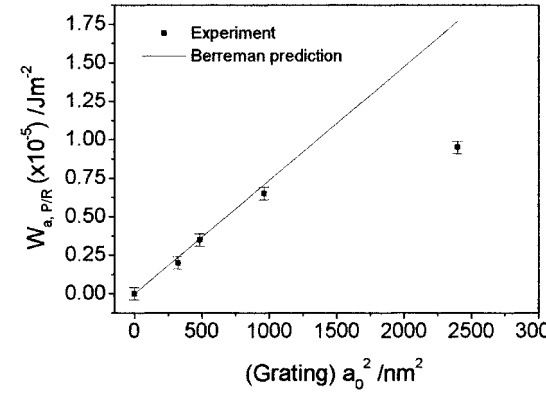

Figure 4. The azimuthal anchoring strength of nematic liquid crystal E7 on a zero order diffraction grating manufactured in photoresist (at a temperature of 21.0°C) as a function of the square of the grating amplitude. Experimental data (symbols) are shown in relation to the theoretical predictions from the Berreman model (solid line).

just as a reference for comparison between the theoretical predictions of the Berreman model and the experimental results.

There is quite good agreement in magnitude between the line and symbols for the shallower gratings, demonstrating that Berreman's model holds for these grating profiles. However, the experimental results can be seen to deviate from Berreman's theoretical predictions progressively more with increasing grating depth. This behaviour can be understood in a number of ways. Firstly, it may be a result of Berreman's model breaking down. Indeed, there is an assumption within the model that the curvature of the deformed directors (which follow the grating surface), and subsequently the strain energy density, can be described by the second derivative of the surface profile. This assumption is only valid for amplitude reliefs with very small depth-to-pitch ratios. Hence, one would expect the agreement between experiment and theory to become progressively worse with increasing groove depth. Unfortunately, implementing a correction to the original model to allow for deep grating profiles is a non-trivial problem, since a new function must be found to describe adequately the curvature of the distorted directors. The function is still required to decay exponentially into the bulk of the liquid crystal, as well as obeying the Laplace equation in the regime where the second derivative approximation is no longer valid. Although a Lambert W function fits these criteria, the result is a set of differential equations which do not admit simple analytical solutions.

An alternative explanation of the results is that the already reduced surface order [6] of the liquid crystal close to the grating surface, becomes increasingly reduced as the grating grooves become deeper. Hence the surface mimics a higher temperature liquid crystal region. This means that the effective twist elastic constant will be a 'surface' elastic constant corresponding to a lower order parameter region than the bulk material. As the grooves become deeper, the surface disorder may further rise, thus making the elastic constant correction term increasingly more significant. Indeed one might imagine the surface disorder to become so severe as to 'melt' the liquid crystal completely in the bottom of the grating troughs, thus decreasing the effective amplitude of the grating profile. This would have the result that the expected increase in anchoring strength with groove depth may not happen, since the groove depth, in effect, is shallowed by filling with disordered material.

The reduced birefringence (Δn) observed at a grating surface by Bryan-Brown *et al.* [6] was of the order of 0.05 and is expected to grow exponentially into the bulk value with increasing distance from the grating surface. Hence any observed changes in the bulk liquid crystal refractive indices at the cell surfaces would be small and highly localized. As mentioned previously, in order to reduce the complexity of the modelling of the short pitch grating surface, the liquid crystal/photoresist interfacial layer has been modelled as a planar layer with refractive indices intermediate between those of the liquid crystal and the photoresist. Since the zero order grating structure also exhibits weak form birefringence [21], this unfortunately renders the observation of any small reduction of birefringence of the liquid crystal within this interfacial region impossible. However, a recent study by the present authors [22] has allowed the surface order of one such grating/rubbed polyimide cell to be probed as a function of temperature. This study provides further evidence of a reduced order parameter at the grating surface (in comparison with the bulk value) and of surface memory effects.

A valid alternative to all of these explanations is that the true nature of alignment on the photoresist grating is not properly understood. The reality of the situation is probably that alignment comes about from a combination of topological effects and molecular effects. Since the grating is manufactured in a photoresist layer it is quite likely there will be some adsorption of liquid crystal molecules into the polymer, thus forming some contribution to the surface physics. As the grating depth increases, the surface area of the grating onto which adsorption may occur increases. It is difficult to guess what effect this may have on the anchoring of the liquid crystal. Certainly, the experimentally determined anchoring strength increases with increasing groove depth, but it is also seen to reach a plateau. This may relate to a condition in which the surface order is the same as the bulk.

4. Conclusions

An optical guided mode technique has been used to probe the distortions in a nematic liquid crystal layer under the application of an in-plane electric field. Alignment of the liquid crystal has been achieved on one surface by a zero order diffraction grating manufactured in photoresist, and on the other by rubbed polyimide. By fitting angle-dependent reflectivity and transmission data to multilayer optical theory, the director profile of the liquid crystal has been accurately determined. Comparing these profiles with those predicted by elastic continuum theory has allowed the twist elastic constant and azimuthal anchoring strengths on the two surfaces to be quantified.

These results have been analysed in the context of the Berreman topological-alignment model. Good agreement was found for shallow amplitude gratings, but not for larger amplitude gratings. The implications of this discrepancy have been discussed. This work highlights the need for a more comprehensive topological model

that allows for both deep grating profiles and a variable elastic constant within the cell. Further, this work demonstrates the potential of non-diffractive diffraction gratings as a means of liquid crystal alignment. The spread of experimentally determined anchoring strengths shown in figure 4 demonstrates the controllable nature of this form of alignment layer. Indeed, the deepest grating in figure 4 corresponds to an anchoring strength that is comparable in magnitude to those of rubbed polyimide [15].

The authors would like to acknowledge the financial support of the Defence Evaluation and Research Agency (Malvern) and the Engineering and Physical Sciences Research Council.

References

[1] Berreman, D. W., 1972, *Phys. Rev. Lett.*, **28,** 1683.
[2] Flanders, D. C., Shaver, D. C., and Smith, H. I., 1978, *Appl. Phys. Lett.*, **32,** 112.
[3] Cheng, J., and Boyd, G. D., 1979, *Appl. Phys. Lett.*, **35,** 444.
[4] Sugimura, A., Yamamoto, N., and Kawamura, T., 1981, *Jpn. J. appl. Phys.*, **20,** 1343.
[5] Kawata, Y., Takatoh, K., Hasegawa, M., and Sakamoto, M., 1994, *Liq. Cryst.*, **16,** 1027.
[6] Bryan-Brown, G. P., Sambles, J. R., and Welford, K. R., 1993, *Liq. Cryst.*, **13,** 615.
[7] Nakamura, M., and Ura, M., 1981, *J. appl. Phys.*, **52,** 210.
[8] Bryan-Brown, G. P., Brown, C. V., Sage, I. C., and Hui, V. C., 1998, *Nature*, **392,** 365.
[9] Bryan-Brown, G. P., Brown, C. V., Jones, J. C., Wood, E. L., Sage, I. C., Brett, P., and Rudin, J., 1997, *SID Dig.*, **28,** 37.
[10] Känel, H. V., Litster, J. D., Melngailis, J., and Smith, H. I., 1981, *Phys. Rev. A*, **24,** 2713.
[11] Newsome, C. J., O'Neill, M., Farley, R. J., and Bryan-Brown, G. P., 1998, *Appl. Phys. Lett.*, **72,** 2078.
[12] Barberi, R., Dozov, I., Giocondo, M., Iovane, M., Martinot-Lagarde, Ph., Stoenescu, D., Tonchev, S., and Tsonev, L. V., 1998, *Euro. Phys. J. B*, **6,** 83.
[13] Wood, E. L., Bradberry, G. W., Cann, P. S., and Sambles, J. R., 1997, *J. appl. Phys.*, **82,** 2483.
[14] Yang, F., and Sambles, J. R., 1999, *J. opt. Soc. Am.*, **B16,** 488.
[15] Hallam, B. T., Sambles, J. R., and Brown, C. V., 1999, *J. appl. Phys.*, **86,** 6682.
[16] Yang, F., Sambles, J. R., and Bradberry, G. W., 1999, *J. appl. Phys.*, **85,** 728.
[17] Hallam, B. T., Yang, F., and Sambles, J. R., 1999, *Liq. Cryst.*, **26,** 657.
[18] Hutley, M. C., 1982, *Diffraction Gratings* (London: Academic Press).
[19] Hallam, B. T., and Sambles, J. R., *J. mod. Opt.* (to be published).
[20] Bancroft, M. S., 1991, PhD thesis, University of Manchester, UK.
[21] Born, M., and Wolf, E., 1980, *Principles of Optics* (New York: Pergamon Press).
[22] Hallam, B. T., and Sambles, J. R., *Phys. Rev. E* (to be published).